

Spin Injection in the Nonlinear Regime: Band Bending Effects

G. Schmidt, C. Gould, P. Grabs, A. M. Lunde,* G. Richter, A. Slobodskyy, and L.W. Molenkamp

Physikalisches Institut (EP3), Universität Würzburg, Am Hubland, 97074 Würzburg, Germany

(Received 14 June 2002; published 4 June 2004)

We report on electrical spin-injection measurements into a nonmagnetic semiconductor in the nonlinear regime. For voltage drops across the interface larger than a few mV the spin-injection efficiency decreases strongly. The effect is caused by repopulation of the minority spin level in the magnetic semiconductor due to band bending at the interface.

DOI: 10.1103/PhysRevLett.92.226602

PACS numbers: 72.25.Dc, 72.25.Hg, 81.05.Dz

Electrical spin injection into semiconductors can be understood [1] using a current-imbalance model originally developed for metals [2]. This model reveals [1] the importance of a conductance mismatch between ferromagnetic metals and semiconductor that precludes spin injection. While in the meantime several methods of avoiding the conductance mismatch have been proposed, by far the most robust route towards spin injection to date [3,4] is the use of dilute II-VI magnetic semiconductors (DMSs) that exhibit the giant Zeeman effect [5], have a conductivity comparable to that of nonmagnetic semiconductors, and can boast spin polarizations close to 100% at a small applied magnetic field. Recently, we used a simple DMS—nonmagnetic semiconductor (NMS) heterostructure [consisting of (Zn,Mn,Be)Se as DMS and lattice matched (Zn,Be)Se as NMS] to demonstrate [4] the magnetic field dependence of the spin-induced boundary resistance, which increases with field as the magnetization of the paramagnetic DMS increases. The experiments reported in Ref. [4] were all done in the regime of linear response, where the current-imbalance model is appropriate.

However, spin-injection experiments in semiconductors allow one to very easily enter the regime of nonlinear response, where corrections to the model of Ref. [1] are necessary. In this Letter we report on spin-injection measurements in the nonlinear regime. We find that a first correction to [1] occurs due to the strong effects that band bending and charge accumulation have on the nonlinear transport. We model the observed phenomena by generalizing Ref. [1] to include these typical semiconductor phenomena, and obtain good agreement with the experiments. It should be noted that the effects found here are of a fundamentally different nature than the drift-induced effects discussed recently by Yu and Flatté [6] (which occur at still larger electric fields [7]).

The devices are all-II-VI semiconductor heterostructure fabricated by molecular beam epitaxy, consisting of three semiconductor layers. From bottom to top these layers are a nonmagnetic *n*-type $\text{Zn}_{0.97}\text{Be}_{0.03}\text{Se}$ layer (thickness 500 nm, $n \approx 10^{19} \text{ cm}^{-3}$), a dilute magnetic $\text{Zn}_{0.89}\text{Be}_{0.05}\text{Mn}_{0.06}\text{Se}$ layer (thickness 100 nm, $n \approx 5 \times 10^{18} \text{ cm}^{-3}$), which acts as a spin aligner, and a top layer of

10 nm highly *n*-doped ZnSe ($n \approx 2 \times 10^{19} \text{ cm}^{-3}$). The latter ensures good quality Ohmic contacts and was covered *in situ* with aluminum. In the Al layer, $200 \times 250 \mu\text{m}$ contact pads were defined and used as a mask for a subsequent wet etching step down to the $\text{Zn}_{0.97}\text{Be}_{0.03}\text{Se}$, leaving only two contacts and the transport layer in between. The resulting sample is schematically shown as an inset in Fig. 1.

The samples were inserted in a magnetocryostat and their transport properties were determined at 1.6, 3, 4.2, and 6 K. The magnetoresistance of the devices was measured using dc techniques and a quasi-four-probe geometry, excluding the wiring resistance of the setup, while still including the contact resistance of the device [8]. For bias voltages V_{bias} in the regime of linear response (300 μV or less) the device showed a positive magnetoresistance. Figure 1 plots the relative magnetoresistance $\Delta R/R$ for a sample with a distance $x_0 = 10 \mu\text{m}$ between the contact pads, taken at 1.6 K, where the zero-field resistance $R = 420 \Omega$. As described in Ref. [4], the magnetoresistance results from the increase of the spin-induced boundary resistance with magnetic field. All

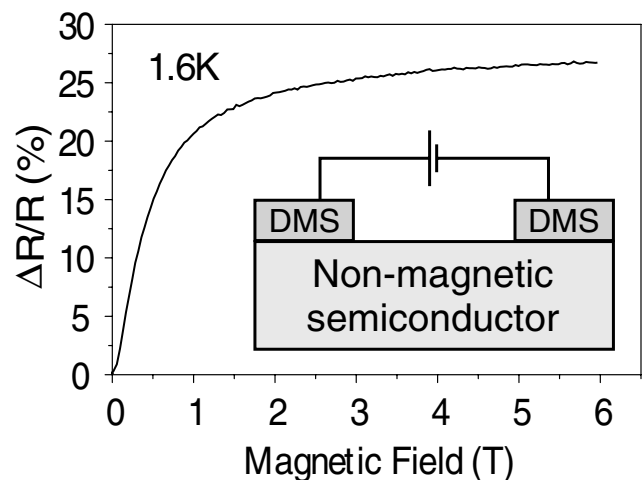


FIG. 1. Inset: spin injection device used in the experiment consisting of a nonmagnetic semiconductor layer with two DMS top contacts. The graph gives the resistance change $\Delta R/R$ versus magnetic field B .

data discussed here were taken on the same sample as in Fig. 1; we verified that the effects discussed occur in samples with varying doping concentrations and dimensions. We found experimentally that both R and the saturated magnetoresistance $\Delta R/R \approx 0.25$ are independent of temperature in the investigated range.

We now leave the regime of linear response and in Fig. 2 plot the current versus V_{bias} curves for the sample at $B = 0$ T, $B = 0.57$ T, where the magnetoresistance is strongly positive, and $B = 3$ T, when the magnetoresistance is well saturated. At first glance, the curves of Fig. 2 appear rather linear and fairly similar; however, a careful inspection shows a crucial difference between the curves, which is put into evidence in the inset of the figure, where we plot the difference in voltage drop between the 0.57 T curve and the $B = 0$ T curve. It is clear that at low currents, an additional voltage drop is observed in the at field curve and that this additional voltage drop vanishes as the current is increased.

The results are easier to view when, instead of current versus V_{bias} plots, we plot the magnetoresistance of the sample. The main experimental result of this Letter is summarized in Fig. 3(a). When the applied voltage is increased, a pronounced and very rapid drop of the magnetoresistance is observed, reducing the effect by 2 or more orders of magnitude on applying a voltage of around 10 mV across the junction. At higher voltages, the device resistance is no longer dependent on the magnetic field, indicating that a reduction of the spin injection is responsible for the effect. The experimental data in Fig. 3(a) were taken starting from three different values of $\Delta R/R$ (i.e., at different values of the magnetic field B) in the linear response regime (i.e., $\Delta R/R \approx 0.05, 0.1,$ and 0.15 , respectively), at the four different temperatures mentioned above. We chose starting points below the saturation

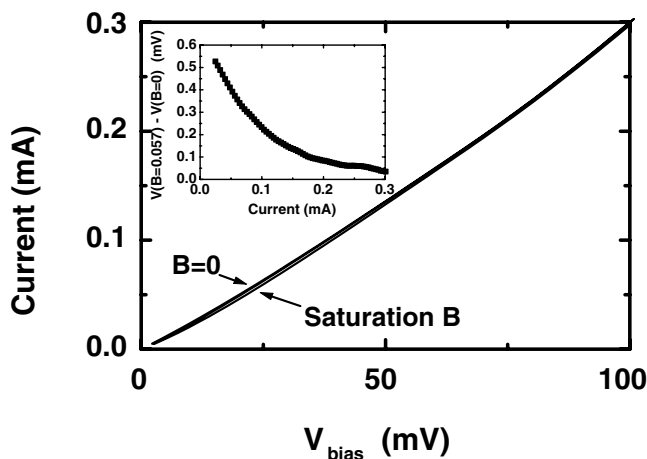


FIG. 2. Current versus voltage curves for the sample in B fields of 0, 0.57, or 3 T. On this scale, the 0 and 0.57 T curves cannot be distinguished. Inset: the difference in voltages between the 0.57 and the 0 T curve is plotted as a function of current, showing that the two curves are, in fact, remarkably different.

tion value of the magnetoresistance because at saturation, the simulations can give only a lower limit for the Zeeman splitting, while below saturation, the Zeeman splitting can be determined exactly.

Obviously, the nonlinearities show a marked temperature dependence. Moreover, while the horizontal axis displays the bias voltage applied to the device, only the drop over the junction V_j (roughly $V_j \approx 0.15V_{\text{bias}}$) contributes to the quenching of the effect, and it is therefore V_j that illustrates the energy scales involved in the nonlinearities. We detail below how V_j is defined and can be calculated from V_{bias} .

The drop of the magnetoresistance can be understood if we combine the model for diffusive spin-polarized transport with the band structure of the semiconductor heterostructure. When a current is driven from a

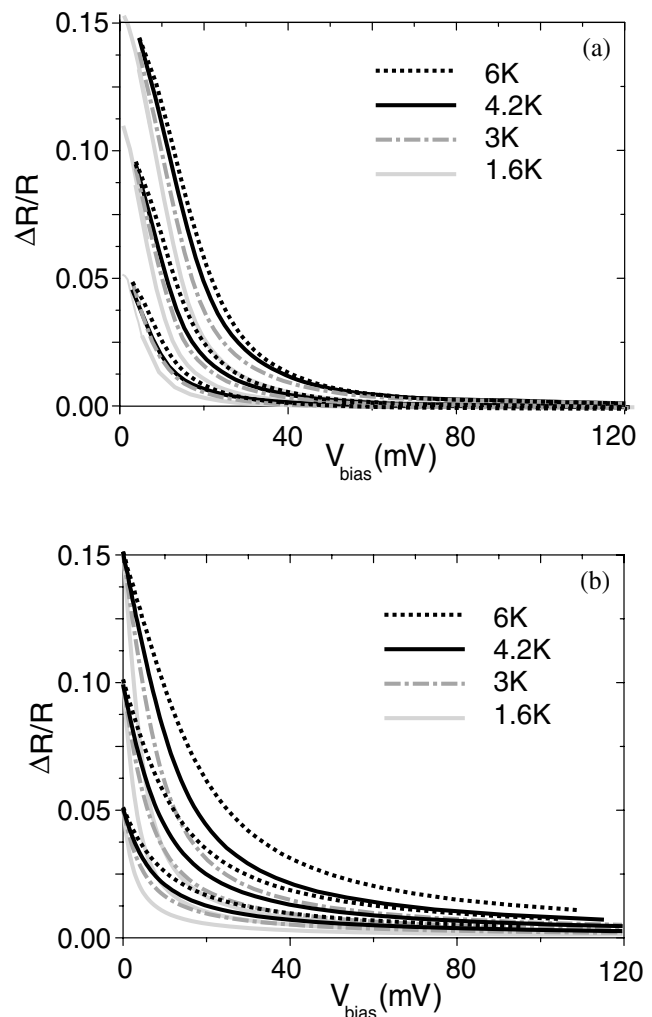


FIG. 3. (a) Experimental and (b) theoretical nonlinear magnetoresistance $\Delta R/R$ data plotted as a function of the applied voltage V_{bias} . (Note that only $V_j \approx 0.15V_{\text{bias}}$ drops over the interface, as described in the text.) To facilitate comparison between experiment and theory, curves are plotted starting at several fixed values of $\Delta R/R$ (obtained by carefully adjusting B), for temperatures of 1.6, 3, 4.2, and 6 K. The parameters involved in the modeling are discussed in the text.

spin-polarized material into a nonpolarized material, the electrochemical potentials for spin-up (μ^\uparrow) and spin-down (μ^\downarrow) split at the interface. In linear response, the length scale of this splitting is given by the spin scattering length of each material. The situation is depicted in Fig. 4, where the Zeeman-split conduction band (full drawn lines) and relevant potentials (dash-dotted lines) of the DMS are shown on the left side of the figure. The interface is indicated by the dotted vertical line at $x = 0$, with the NMS in the right half of the plane. The splitting of μ^\uparrow and μ^\downarrow is the driving force which leads to a spin-polarized current in the nonmagnetic material. Because the conductivities for spin-up and spin-down are equal in the NMS, only a difference in the derivative of the electrochemical potential can lead to different currents in both spin channels. Since the *electrical* potential must

be equal for both spin directions, this difference can be introduced only through the *chemical* potential, i.e., by spin accumulation. Spin injection thus leads to a potential drop at the interface which drives the spin conversion. This voltage drop, which may alternatively be regarded as a spin-induced boundary resistance, is indicated in Fig. 4 by the potential difference at $x = 0$ between the thin drawn lines, denoted $\mu_{\text{DMS}}^{\text{av}}$ and $\mu_{\text{NMS}}^{\text{av}}$, that depict the conductivity-weighted average of the electrochemical potential in DMS and NMS, respectively.

While in the NMS the splitting of the Fermi levels is symmetrical because the conductivities for spin-up and spin-down electrons are identical, in the DMS, the splitting for the majority- [$c^\uparrow \equiv \mu_{\text{DMS}}^\uparrow(0) - \mu_{\text{DMS}}^{\text{av}}(0)$] and minority- [$c^\downarrow \equiv \mu_{\text{DMS}}^{\text{av}}(0) - \mu_{\text{DMS}}^\downarrow(0)$] spin electrons can, in one dimension, be expressed as [4,9]

$$c^\uparrow, c^\downarrow = -\frac{\lambda_{\text{N}}}{\sigma_{\text{N}}(1 + e^{-x_0/\lambda_{\text{N}}} + 2(\lambda_{\text{N}}/x_0)e^{-x_0/\lambda_{\text{N}}}) + (\lambda_{\text{N}}\sigma_{\text{D}}/\sigma_{\text{N}}\lambda_{\text{D}})(1 - \beta^2)}, I\beta(\beta \pm 1) \quad (1)$$

where in the numerator the plus (minus) sign applies to c^\uparrow (c^\downarrow), respectively. In Eq. (1), λ_{D} , λ_{N} , σ_{D} , σ_{N} are the spin flip length and the conductivity in the DMS and the NMS, respectively, x_0 is the spacing between the contacts, I is the current, and β is the degree of spin polarization in the bulk of the contacts. Note that c^\uparrow and c^\downarrow are defined setting $\mu_{\text{DMS}}^{\text{av}}(0)$ as the reference level for the energy scale; i.e., $\mu_{\text{DMS}}^{\text{av}}(0) = 0$. For the potential drop ΔU at the interface, and the resulting magnetoresistance, we simply have

$$e\Delta U = \mu_{\text{DMS}}^{\text{av}}(0) - \mu_{\text{NMS}}^{\text{av}}(0) = (c^\uparrow + c^\downarrow)/2, \quad (2a)$$

$$\Delta R = \Delta U/I, \quad (2b)$$

where e is the fundamental charge. Equations (1) and (2) are quite general and describe spin injection in metals as well as semiconductors—but only in the linear regime. The magnitude of the Fermi-level splitting (and thus of ΔU) is different for different types of junctions: since the spin-polarized current is driven solely by the spin accumulation, the Fermi-level splitting has to be of the order of the current imbalance between the spin channels times the resistivity of the normal metal. When magnet and nonmagnet are both semiconductors as in the present experiment, the splitting can easily be in the range of mV. This implies that in a spin-injecting DMS the Fermi energy, the Zeeman splitting and the Fermi-level splitting are all in the range of mV, and nonlinear effects are to be expected for bias of similar magnitude.

This situation, applied to the present experiment, is pictured in some detail in Fig. 4. The conduction band of the NMS is some tens of mV below that of the DMS, which is split by the Zeeman energy into two subbands, $E_{\text{C}\uparrow}^{\text{DMS}}$ and $E_{\text{C}\downarrow}^{\text{DMS}}$. From previous spin-injection experiments [3,4] and from spin flip Raman scattering we know that the DMS is fully spin polarized at low temperatures and moderate magnetic fields, which recent band structure calculations understand as resulting from

the formation of an impurity band [10]. This implies that the Fermi energy is situated above the lower and at least a few mV below the upper Zeeman level.

As discussed above, spin injection will lead to the occurrence of a “built-in potential” ΔU at the interface. This is an actual electrochemical potential step (i.e., not spin dependent). In order to preserve both charge conservation and the band offset at the junction, ΔU has to be compensated by band bending and charging at the interface. In Fig. 4, this is indicated by the dashed lines emanating from $E_{\text{C}\uparrow}^{\text{DMS}}$ and $E_{\text{C}\downarrow}^{\text{DMS}}$. (In principle, one also expects band bending at the NMS side of the junction. For clarity, we have not included this in Fig. 4, nor in

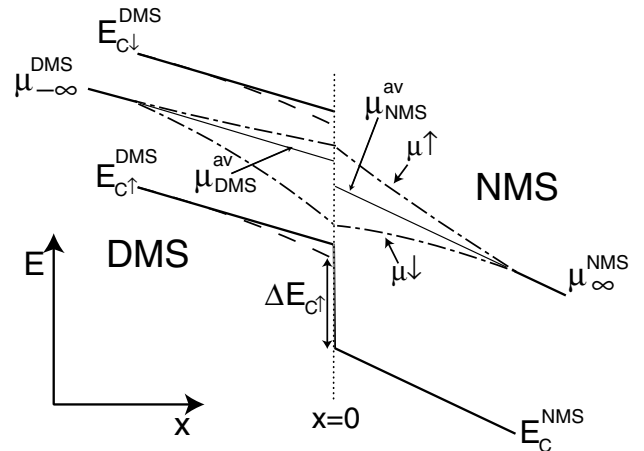


FIG. 4. Diagram of the band bending at the spin-injecting DMS/NMS interface. $\Delta E_{\text{C}\uparrow}$ denotes the location of the conduction band offset between $E_{\text{C}\uparrow}^{\text{DMS}}$ and $E_{\text{C}}^{\text{NMS}}$ when band bending is taken into account; all other symbols are discussed in the text. Note the discontinuity between $\mu_{\text{DMS}}^{\text{av}}$ and $\mu_{\text{NMS}}^{\text{av}}$ at the junction ($x = 0$), which is the potential difference ΔU in Eqs. (2).

the modeling we describe below. Its inclusion is straightforward.)

It is now obvious that the spin-injection process can be seriously affected by any strong band bending, as must occur at higher current levels. At the interface, the majority spin electrochemical potential μ^\uparrow then approaches the upper Zeeman level $E_{\text{Cl}}^{\text{DMS}}$, thus reducing the spin polarization β in the DMS close to the interface. β being close to 1, however, is a prime prerequisite for injecting a highly spin-polarized current into the NMS [1]. We can thus expect the spin injection (and thus the magnetoresistance) to collapse as soon as the band bending starts to reduce β .

Since β and ΔU depend on each other, a modeling of the phenomena as a function of V_{bias} should be done in a self-consistent manner. One can avoid a recursive calculation when starting from a given value of $\Delta R/R$ in the linear response regime (this is the main reason for presenting the data emanating from the same $\Delta R/R$ value in Fig. 3.) We first use Eqs. (1) and (2) to calculate the bulk polarization β in the DMS. In the linear regime, the bulk value of β equals $\beta(x=0)$, the spin polarization at the interface. Assuming Boltzmann statistics, we then directly have the energy splitting between $E_{\text{Cl}}^{\text{DMS}}(0)$ and $\mu^\uparrow(0)$ from

$$\beta(x=0) = \tanh\left[\frac{E_{\text{Cl}}^{\text{DMS}}(0) - e\Delta U - \mu^\uparrow(0)}{2k_{\text{B}}T}\right], \quad (3)$$

where $\Delta U = 0$ for infinitesimally small bias. For modeling the dependence on V_{bias} , we gradually increase ΔU (note that here we assume all band bending to occur in the DMS), calculate the reduced $\beta(x=0)$ using Eq. (3), and substitute this value for the bulk polarization in Eqs. (1) and (2) to calculate $\Delta R/R$. At the same time, ΔU can be converted in a voltage drop across the junction, V_j .

The latter quantity is conveniently accessible for comparison with the experiment. This is because $\Delta R \rightarrow 2\lambda_{\text{N}}/\sigma_{\text{N}}$ for $B, (x_0/\lambda_{\text{N}}) \rightarrow \infty$, as can easily be verified from Eqs. (1) and (2). Experimentally, we have (within our one-dimensional modeling) $\sigma_{\text{N}} = 2.5 \times 10^{-4} \Omega^{-1} \text{cm}$, yielding $\lambda_{\text{N}} = 1.25 \mu\text{m}$. For comparing the experimental [Fig. 3(a)] and theoretical [Fig. 3(b)] plots of the nonlinear behavior, we may now calibrate the voltage axis according to $V_j = I\Delta R + V_{\text{bias}}(\lambda_{\text{N}}/x_0)$.

As to the remaining parameters, we have from experiments on single DMS layers that σ_{D} , converted to one dimension, equals $1.0 \times 10^{-4} \Omega^{-1} \text{cm}$. The only free parameter now left in the model is λ_{D} . Since there is no easy method to measure λ_{D} , and moreover its magnetic field dependence is unknown, the ratio $\lambda_{\text{N}}\sigma_{\text{D}}/\sigma_{\text{N}}\lambda_{\text{D}}$ in Eq. (1) cannot be precisely determined. However, since it is of order unity, and given that the fitting does not strongly depend on the exact value of this ratio, we simply set it equal to 1, yielding $\lambda_{\text{D}} = 0.5 \mu\text{m}$.

The modeling of the band bending effect as described above leads to the plots shown in Fig. 3(b). We find that indeed a few mV of voltage drop across the junction are enough to reduce the spin polarization of the injected current to almost zero. The computed curves closely resemble the experimental results in shape, magnitude, voltage range, and temperature dependence.

At this point, we should address the drift effects introduced by Yu and Flatté [6], which also can induce a reduction of $\Delta R/R$ in our experiments. For the highly (i.e., above the metal-insulator transition) doped samples used here, one can show that drift effects occur only for much higher electric fields than those used here [7]. Moreover, within the drift model one would not expect any temperature dependence for degenerate semiconductors, again in contradiction with the experiments.

In conclusion, we have shown that when spin injection into semiconductors is used beyond the regime of linear response, band bending in the spin-injecting junction can strongly reduce the spin-injection efficiency. Appropriate tailoring of the band structure may be able to circumvent the problems described here.

We acknowledge the financial support of the BMBF, of the DFG (SFB 410), and of the DARPA SPINS program. We thank V. Hock for device fabrication and I. D'Amico, M. Flatté, K. Flensberg, and E. Rashba for useful discussions.

*Present and permanent address: Ørsted Laboratory, Niels Bohr Institute, DK-2100 Copenhagen, Denmark.

- [1] G. Schmidt, D. Ferrand, L.W. Molenkamp, A.T. Filip, and B.J. van Wees, *Phys. Rev. B* **62**, R4790 (2000).
- [2] P.C. van Son, H. van Kempen, and P. Wyder, *Phys. Rev. Lett.* **58**, 2271 (1987); M. Johnson and R.H. Silsbee, *Phys. Rev. B* **35**, 4959 (1987); *Phys. Rev. Lett.* **60**, 377 (1988).
- [3] R. Fiederling, M. Keim, G. Reuscher, W. Ossau, G. Schmidt, A. Waag, and L.W. Molenkamp, *Nature (London)* **402**, 787 (1999).
- [4] G. Schmidt, G. Richter, P. Grabs, D. Ferrand, and L.W. Molenkamp, *Phys. Rev. Lett.* **87**, 227203 (2001).
- [5] J. K. Furdyna, *J. Appl. Phys.* **64**, R29 (1988).
- [6] Z. G. Yu and M. E. Flatté, *Phys. Rev. B* **66**, 235302 (2002).
- [7] I. D'Amico and G. Vignale, *Phys. Rev. B* **69**, 165305 (2004).
- [8] A true four-probe measurement technique is not possible for any sample bigger than the spin flip length in the material, since the voltage leads would be located in a region where the spin splitting has already relaxed.
- [9] G. Schmidt and L.W. Molenkamp, *Semicond. Sci. Technol.* **17**, 310 (2002).
- [10] K. Sato and H. Katayama-Yoshida, *Jpn. J. Appl. Phys.* **40**, L651 (2001).